The improvement of steel properties using Al_2O_3 coatings deposited by plasma spraying

M L Benea[1] and L P Benea[2]

[1] Politehnica University of Timisoara, Department of Engineering and Management, Hunedoara, Romania
[2] Univ. Grenoble Alpes, CNRS, Grenoble INP, IMEP-LAHC 38016 Grenoble, France

E-mail: laura.benea@fih.upt.ro

Abstract. It is well-know that the numerous functions of use of materials can be realized at a high level of performance by using plasma jet coatings, with the reduction of the consumption of important strategic metals. These are determined by the excellent resilience to extreme temperatures, corrosion and wear of the coatings.
This paper aims to characterize coating layers based on Al_2O_3 realized by plasma jet spray by examining its hardness, thermal shock resistance, traction resistance.

1. Introduction

The research and manufacturing of ceramic coatings had gained great attention due to their excellent characteristics and potential applications. Most of ceramic material presenting useful features such as low density, excellent wear resistance, high inertness, high stability and high temperature strength [1], [2]. These features resulted by high atomic strength of ceramic that led to its great hardness, strength and stiffness. Ceramics also possess high resistance to oxidation as well as corrosion in extreme condition and thus make them having a wide range of applications especially in structural and engineering fields [3-5].

Thermal spraying process has been used successfully to produce a range of protective coatings for wear, erosion and heat resistance, as well as restoration of worn parts [6-8]. Especially, oxide ceramics such as Al_2O_3 ceramic coatings, having superior hardness, chemical stability and refractory character, are commonly utilized to resist wear by friction and solid particle erosion [9], [10]. However, plasma-sprayed coatings built up from the successively immediate solidification of the liquid or partially melted droplets onto target substrate typically present weak interface between splats and irregular reticula of microcracks and pores running through it [8], [11]. The porosity and weak interface adversely affect the wear property and the cracks allow corrosive substance in the environment to attach the protective coating. In addition, these ceramic coatings are also vulnerable to thermal fatigue and delamination under mechanical load for its intrinsic brittleness. So, the application of plasma-sprayed Al_2O_3 coating are restricted in many industrial fields such as wear and erosion resistance, especially under increasingly severe conditions by the combination of intrinsic brittleness and microstructural defects [9], [12].

In this work, alumina-titania ceramic coatings were obtained by atmospheric plasma spraying using commercial powders. The powders were characterized before deposition. Relevant properties were determined for the coatings with Metco 101: adhesion, hardness, heat shock resistance.

2. Materials and methods

2.1. Plasma spraying conditions

The principle of plasma spraying is shown schematically in Figure 1. A high frequency arc is ignited between an anode and a tungsten cathode. The gas flowing through between the electrodes (i.e., He, H_2, N_2 or mixtures) is ionized such that a plasma plume several centimetres in length develops. The temperature within the plume can reach as high as 16000K. The spray material is injected as a powder outside of the gun nozzle into the plasma plume, where it is melted, and hurled by the gas onto the substrate surface.

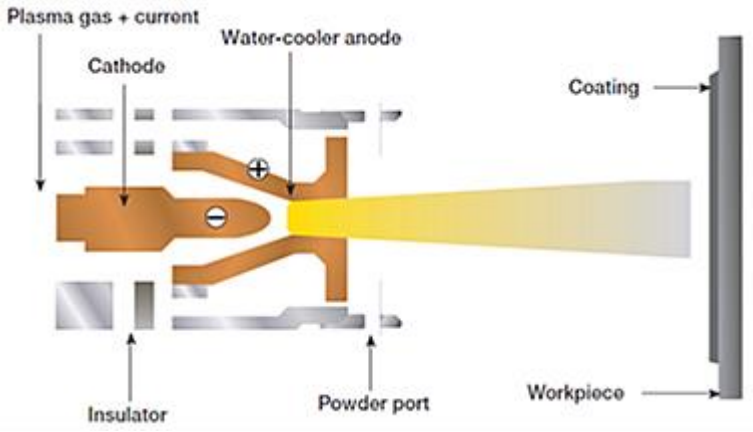

Figure 1. Schematic diagram of the plasma spray process [13]

The deposits of aluminium oxide (METCO 101) were made on a 7M installation and with a low power spray generator, for thermal shock resistance determinations.

For Metco 101 powder, the operating conditions are:

- Parameters of the 7M spraying gun:
    - Primary plasma gas:
        - Argon:
            - Pressure (MPa):0,69
            - Volume (m^3): 2,26
    - secondary plasma gas:
        - Hydrogen:
            - 0,345 MPa pressure
            - 0,78 m^3 debit
    - Intensity of the current at the generator: 500 A and 60-70 V voltage
    - Spraying distance: 60 mm.
- Parameters of the GPPR-400 generator:
    - Plasma jet current: 500 A
    - Plasma gas flow: 2000L/min
    - Spray distance: 50 mm
    - Voltage in the plasma jet: 70 V
    - Transport gas flow: 600 L/min.

Other operating parameters include transversal speed and spraying distance. The jet that is for a sample at a certain distance, which is not usually critical, must be kept constant for a

given application. The distance from which the spray is made will, of course, affect the temperature of the sample.

Figure 2 shows the relationship between spray distance and deposition efficiency for alumina (METCO 101).

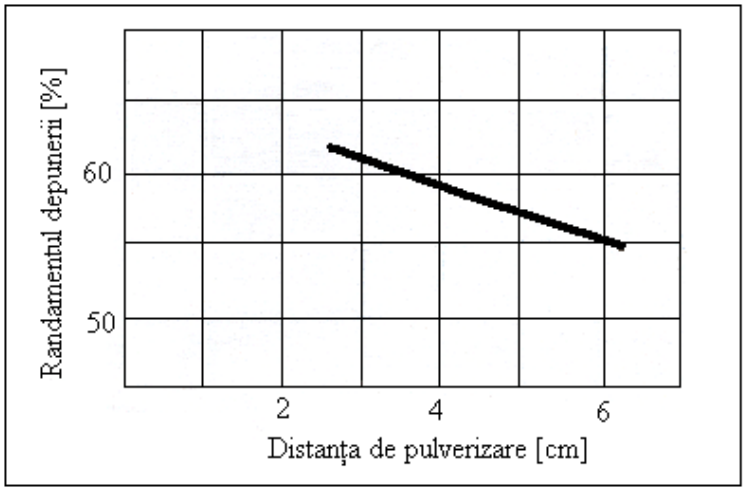

Figure 2. The relationship between spraying distance and deposition efficiency for alumina (METCO 101) [14]

The cross-sectional velocity of the jet over a sample is not usually a critical parameter for plasma jet coatings. More spraying passes are required to obtain thick coatings so that they become homogeneous and avoid exfoliation. A good rule of thumb is that a maximum of 10 microns is applied to a pass. If it is desired to obtain a layer thicker than 10 microns, it is advisable to make two or more successive passes.

2.2. Materials

To characterize the aluminium oxide coatings made in plasma jet, the martensitic stainless steel Z12CNDV12 was used as substrate, whose chemical composition is shown in Table 1.

Table 1. Characteristics of martensitic stainless steel Z12CNDV12

	C	Si	Mn	S	P	Cr	Ni	Mo	V	N_2
Chemical	0,06	≤	0,50	≤	≤	11,0	2,00	1,50	0,25	0,02
composition	0,15	0,35	0,90	0,025	0,035	12,5	3,00	2,00	0,40	0,04

For the resistance to thermal shock, the coating with Al_2O_3, was made on a 25Cr20Ni steel, intended for gas turbines, with a width of 11.5 × 11.5 × 55 mm^3. Sample preparation was done by blasting.

The powder used for plasma jet coating is Metco 101.

The phase composition of the powder used was determined using RX spectra made with a RX DRON 3 diffractometer, using CuKα radiation with wavelength λ = 1.54178 Å, at a voltage of 30 kV and an intensity of 30 mA. The displacement speed of the detector was 1 deg/min.

2.3. Coating characterisation techniques

The determination of the Vikers hardness consists of applying to the test piece, with a force of 2.94 N, for a specific time, of a square diamond square-based pyramidal indenter, with the angle between two

opposite sides of 136°. Vickers hardness is the ratio of the applied load and the size of the surface of the pyramidal trace, which remains on the test piece after the indenter removal [15].

The tensile adhesion is a size that characterizes the unit force required to detach the thermal spray layer from the substrate or the buffer layer, or essentially the force required to detach the layer as a unitary element from the substrate.

Tensile testing is a quasi-direct measure of grip strength. A large number of measurements must be made, knowing the dispersion of the measurement results. The device used is shown in Figure 3 [16].

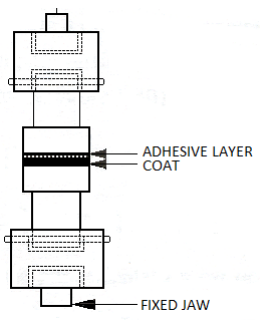

Figure 3. The static method of determining the adhesion of the sprayed coatings

2.3.1.Thermal shock testing for the coats made by using the Metco 101 powder on 25Cr20Ni steel, consist in: fast heating to 800°C in 10 s (or 500°C) and immediate water cooling (600°C/s)without maintaining the maximum temperature.

2.3.2. The model of Takeuchi for calculation of residual stresses in plasma sprayed ceramic coatings. The formation of residual strains in plasma sprayed ceramic and metallic coatings is a very complex process. Several factors, such a substrate material, substrate thickness, physical properties of both the substrate and coating material, deposition rate, relative velocity of the plasma torch, etc., determine the final residual stress state of the coating.

The model of Takeuchi [17] takes primary cooling into account by introducing a strain term ε_e, representing strains in the coating caused by primary cooling. The Takeuchi model uses a uniform substrate temperature and assumes that the entire coating is deposited in one pass.

The stress in the coating at elevated substrate temperature is describe by the following equation (1).

$$\sigma_c(ed, x, T_s) = E_c \cdot \left[\left(\frac{E_c \cdot x + E_s \cdot es}{E_c \cdot ed + E_s \cdot es} \right)^{\varepsilon_e} (1 + \varepsilon_e) - 1 \right] \quad (1)$$

Where:
x: position in coating [m]
Ec: Young's modulus coating [Pa]
Es: Young's modulus substrate [Pa]
ts: thickness of substrate [m]
tc: thickness of coating [m]
ε_e: strain in coating due to primary cooling [-]
Ts: substrate temperature [K].
According to Takeuchi, the strain ε_e, caused by primary cooling equals:

$$\varepsilon_e = \alpha_c (T_m - T_s) \quad (2)$$

Where:
α_c: coefficient of thermal expansion coating
Tm: melting point coating material.

When the stress, caused by primary cooling, exceeds the yield of tensile strength of the coating material, ε_e has to be derived from the stress strain curve of that material.

After cooling down to room temperature, the stress in the coating is equal to:

$$\beta = \frac{1-\alpha_c(T_s -}{1-\alpha_s(T_s -}\sigma_c(ed, x, T_s) = E_c\left[\frac{(1+\varepsilon_e)(\gamma+1)}{\beta+(\gamma+1)^{(1+\varepsilon_e)}-1}\left(\frac{E_c \cdot x}{E_s \cdot es}+1\right)^{\varepsilon_e}-1\right] \quad (3)$$

With:
T_s: substrate temperature [K]
T_r: room temperature [K]
ε_s: coefficient of thermal expansion substrate [K^{-1}].

3. Results and discussion

3.1. Powder characterization

The powder used for plasma jet coating is Metco 101, which contains 97% Al_2O_3 and 3% TiO_2. Particle sizes range from 30-75µm and have a density of 3.5 g/cm^3.

The RX spectrum of Metco 101 powder is shown in Figure 4.

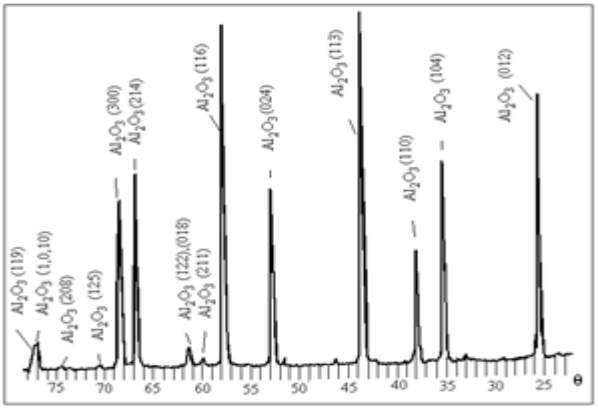

Figure 4. RX spectrum for the Metco 101 powder

3.2. Characterization of ceramic coatings made of aluminium oxide

The coatings METCO 101 made by plasma spray, have:

- Tensile strength between 45-50 MPa;
- VickersHV 0.3 micro-hardness between 680-750 N/mm²

3.2.1. Thermal shock resistance. Table 2 presents some results obtained on the samples coated with a layer of Metco 101 Al_2O_3, with a thickness of 0.3 mm.

Table 2. The results of the thermal shock resistance determination on samples covered with Metco 101 Al_2O_3

Sample code	Number of cycles	T_{max}cycle [°C]	Cooling medium	Obsercations
19	50	800	water	Samples are exfoliated
21	62	800	water	Samples are exfoliated
29	65	800	water	Samples are exfoliated
Average			59	
35	205	500	water	Samples are not exfoliated

Figure 5 presents images of the samples made using the Metco 101 powder coatings at different stages of the experiment. As it can be seen in Figure 5, the samples in the deposited state do not show visible cracks with the naked eye or the optical microscope at usual magnifications.

After 22 cycles, a fine network of cracks consisting of isolated and branched cracks was observed. The branch crack network developed during the following sets of 20 cycles, but unlike the deposition made with TiO2 powders, there was no exfoliation of the coating layer [18].

Because apparently the severity of the heat shock to which the Metco 101 powder coated samples were subjected was too high, a new set of tests was prepared on which thermal shock tests were performed with the maximum cycle temperature of 500 °C, in the same heating and cooling conditions. After performing 205 cycles, the appearance of exfoliation on the surface of the deposits was still not observed.

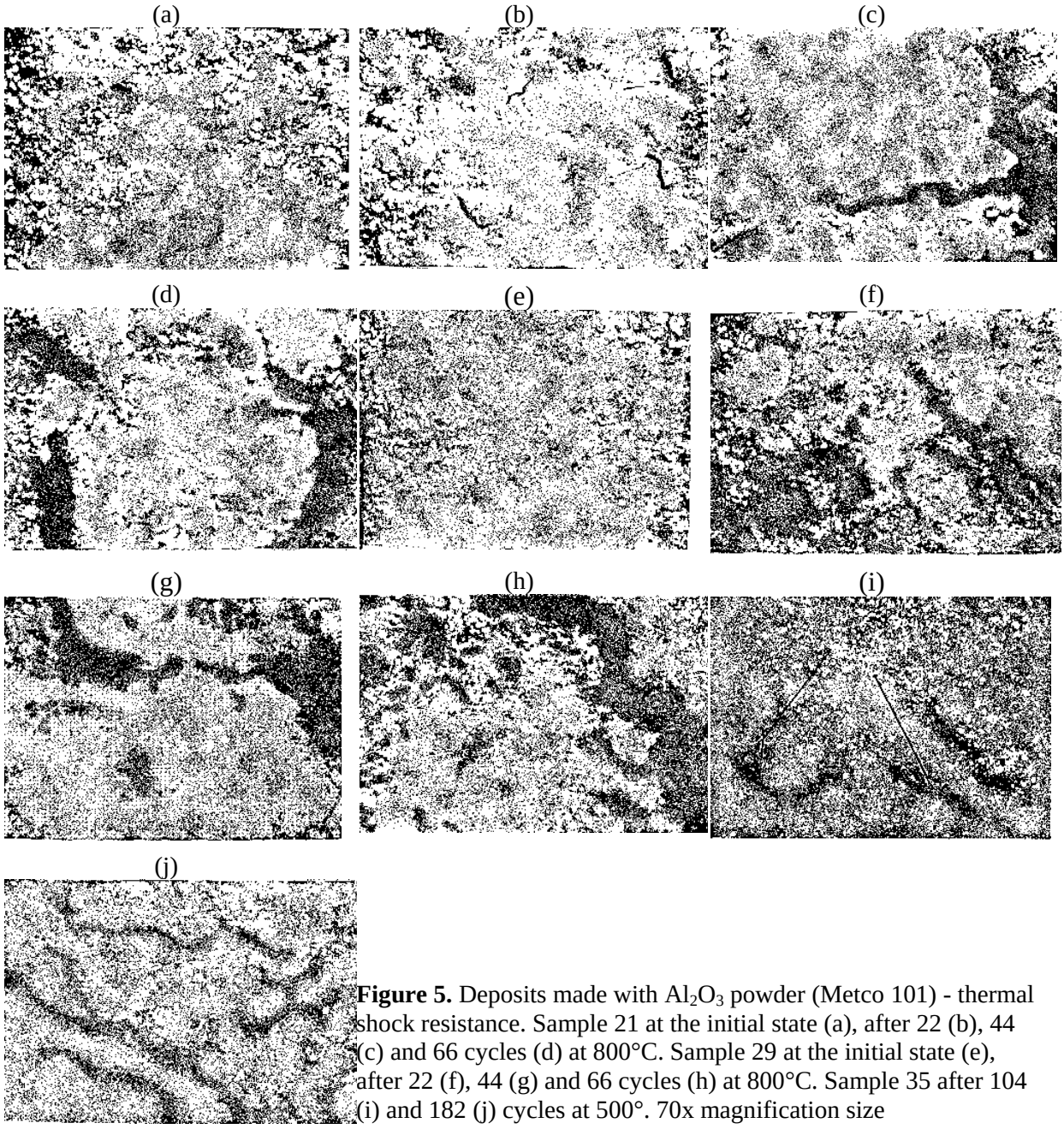

Figure 5. Deposits made with Al_2O_3 powder (Metco 101) - thermal shock resistance. Sample 21 at the initial state (a), after 22 (b), 44 (c) and 66 cycles (d) at 800°C. Sample 29 at the initial state (e), after 22 (f), 44 (g) and 66 cycles (h) at 800°C. Sample 35 after 104 (i) and 182 (j) cycles at 500°. 70x magnification size

From the literature, the necessary constants for calculating the tensile stress inside the coating layers were extracted for aluminium oxide. They are presented in Table 3.

Table 3. Constants needed to calculate the stress in the coating layers according to Takeuchi's method

Constant	Al_2O_3 Z12CNDV12
α_c	$8 \cdot 10^{-6}$
α_s	$1,2 \cdot 10^{-5}$
e_d	10^{-4}
e_s	$1,5 \cdot 10^{-3}$
E_s	$780 \cdot 10^{6}$
E_c	$100 \cdot 10^{6}$
T_m	2323
T_s	423
T_r	293
x	$0\text{-}10^{-4}$

The processing of these data was realized in Matlab and is shown in Figure 6.

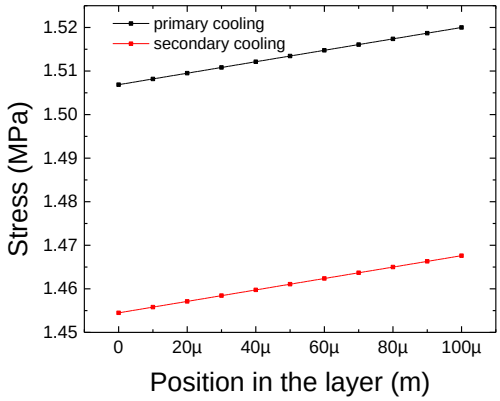

Figure 6. Variation of stresses in the coating layer realized with METCO 101 powder

4. Conclusions

The phase composition of Metco powder was determined by X-ray diffraction spectrum, which shows that it contains crystallized aluminium oxide in the rhombohedral system.

By analysing the results of the Vickers microhardness determinations for the Metco 101 powder coating, we can conclude that it has a high hardness.

The determination of adhesion using static methods, in the coating layers made with aluminium oxide, leads to the following conclusion: tensile strength is high, for these coating layers there is no need for a cling layer, because they have high adhesion to the martensitic stainless steel substrate.

The analysis of the results of determining the thermal shock resistance of the Al_2O_3 deposits led to the following conclusions: (1) the samples in the deposited state do not show visible cracks with the open eye or the optical microscope at usual magnifications; (2) after 22 cycles at a maximum temperature of 800°C, a fine network of cracks consisting of both isolated and branched cracks is observed; (3) during the following sets of 20 cycles at a maximum temperature of 800°C, the network

of branched cracks develops, but there is no exfoliation of the coating layer; (4) at a temperature of the thermal cycle of 500°C, after performing 205 cycles, the appearance of the exfoliation on the surface of the deposits was not observed.

Calculating the stresses that appear in the coating layers using Takeuchi's method, leads us to the conclusion that in the coating layer made with aluminium oxide powder (Metco 101) the value of the stresses is higher than in the deposit made with TiO_2 (Metco 102) [18]. This is easy to understand because Al_2O_3 has a coefficient of thermal expansion greater than TiO_2. On the same martensitic stainless steel substrate, the difference between the coefficients of thermal expansion of the layer and the substrate is greater in the case of aluminium oxide and therefore the stress is greater.

References

[1] Xing Y, Deng J, Feng X and Yu S 2013 Effect of laser surface texturing on Si_3N_4/TiC ceramic sliding against steel under dry friction, *Materials & Design* **52** 234-245
[2] Samant A N and Dahotre N B 2009 Laser machining of structural ceramics—A review, *Journal of the European Ceramical Society* **29** 969-993
[3] Herman H, Berndt C C, Wang H, Wachtma J B and Haber R A 1993 *Ceramic Films and Coatings* Noyes Publications, Park Ridge, NJ, USA
[4] Günen A 2016 Micro-Abrasion Wear Behavior of Thermal-Spray-Coated Steel Tooth Drill Bits *Acta Phys. Pol. A* **130** 217-222
[5] Karahan I H 2016 Corrosion Properties of AISI 4140 Industrial Steels Coated with Aniline in Different Storage Conditions, *Acta Phys. Pol. A* **130** 286-288
[6] Westergard R, Erickson L, Axen N, Hawthorne H M and Hogmark S 1998 The erosion and abrasion characteristics of alumina coatings plasma sprayed under different spraying conditions, *Tribol. Int.* **31** 271-279
[7] Haessler W, Thielsch R and Mattern N 1995 Structure and electrical properties of PZT thick films produced by plasma spraying, *Mater. Lett.* **24** 387-391
[8] Li J F, Huang J Q, Tan S H, Cheng Z M and Ding C X 1998 Tribological properties of silicon carbide under water-lubricated sliding, *Wear* **218** 167-171
[9] Hawthorne H M, Erickson L C, Ross D, Tai H and Troczynski T 1997 The microstructure dependence of wear and indentation of some plasmasprayed alumina coatings, *Wear* **203-204** 709-714.
[10] Ramachandran K, Selvarajan V, Ananthapadmanabhan P V and Screekumar K P 1998 Microstructure, adhesion, microhardness, abrasive wear resistance and electrical resistivity of the plasma sprayed alumina and aluminatitania coatings, *Thin Solid Films* **315** 144-152
[11] Mcpherson R 1981 The relationship between the mechanism of formation, microstructure and properties of plasma-sprayed coatings, *Thin Solid Films* **83** 297-310
[12] Pantelis D I, Psyllaki P and Alexopoulos N 2000 Tribological behaviour of plasma-sprayed Al_2O_3 coatings under severe wear conditions, *Wear* **237** 197-204
[13] Oerlikon Metco 2016 *An Introduction to Thermal Spray*, pp 9
[14] ***ASM International 2004 *Handbook of Thermal Spray Technology*,
[15] Kingery W D 1955 Affecting Thermal Stress Resistance of ceramic materials, *J.Am.Ceram.Soc.* **38**(1) 3-15
[16] ***European Committee 1993 *Thermal Spraying. Determination of tensile adhesive strength. European Standard CEN/TC 240 N 53*
[17] Takeuchi S, Ito M and Takeda K 1990 Modelling of residual stress in plasma-sprayed coatings: Effect of substrate temperature, *Surface and Coatings Technology* **43** 426-435
[18] Benea M L and Benea L P 2016 Characterisation of the TiO_2 coatings deposited by plasma spraying, *IOP Conf. Ser.: Mater. Sci. Eng.* **106** 012024